12-15-2008

Transport-based Dopant Metrology in Advanced FinFETs

Gabriel P. Lansbergen
Kavli Institute of Nanoscience, Delft University of Technology

Rajib Rahman
Network for Computational Nanotechnology, Birck Nanotechnology Center, Purdue University

Cameron J. Wellard
Center for Quantum Computer Technology, University of Melbourne

Jaap Caro
Kavli Institute of Nanoscience, Delft University of Technology

Nadine Collaert
InterUniversity Microelectronics Center

See next page for additional authors

Follow this and additional works at: http://docs.lib.purdue.edu/nanodocs

Part of the Nanoscience and Nanotechnology Commons

Authors

Gabriel P. Lansbergen, Rajib Rahman, Cameron J. Wellard, Jaap Caro, Nadine Collaert, Serge Biesemans, Gerhard Klimeck, Lloyd C. L. Hollenberg, and Sven Rogge

Transport-based dopant metrology in advanced FinFETs

Gabriel P. Lansbergen[1], Rajib Rahman[2], Cameron J. Wellard[3], Jaap Caro[1], Nadine Collaert[4], Serge Biesemans[4], Gerhard Klimeck[2,5], Lloyd C.L. Hollenberg[3], Sven Rogge[1]

[1] Kavli Institute of Nanoscience, Delft University of Technology, The Netherlands, [2]Network for Computational Nanotechnology, Birck Nanotechnology Center, Purdue University, USA, [3]Center for Quantum Computer Technology, School of Physics, University of Melbourne, Australia [4]InterUniversity Microelectronics Center (IMEC), Belgium, [5]Jet Propulsion Laboratory, Caltech, USA

Abstract

Ultra-scaled FinFET transistors bear unique fingerprint-like device-to-device differences attributed to random single impurities. Through correlation of experimental data with multimillion atom simulations in NEMO 3-D, we can identify the impurity's chemical species and determine their concentration, local electric field and depth below the Si/SiO$_2$ interface. The ability to model the excited states rather than just the ground states is the critical need. We therefore demonstrate a new approach to atomistic impurity metrology and confirm the assumption of tunneling through individual impurity quantum states.

Introduction

Advanced Si MOSFET devices have shrunk to dimensions where individual impurities in the channel region can dominate device characteristics. Due to the random nature of the impurity distribution, parameters like threshold voltage and leakage current show device-to-device fluctuations (1). An atomistic point of view is imperative to understand and determine the underlying donor characteristics in the channel. Several recent experiments have showed that the fingerprint of a single dopant can be identified in low-temperature transport through such devices (2-4), providing a new method to characterize devices down to the level of a single impurity. In the context of state control in quantum computing it was shown that in conjunction with multi-million atom modeling, one can determine a donors chemical species, local electric field and depth below the interface (4). Here we show that the aforementioned technique can be used to perform single donor mapping in advanced Si FinFETs. By carefully examining the fingerprints of isolated donors in an ensemble of devices, we can determine the chemical species, concentration, and local field of donors in the channel region in a non-destructive fashion.
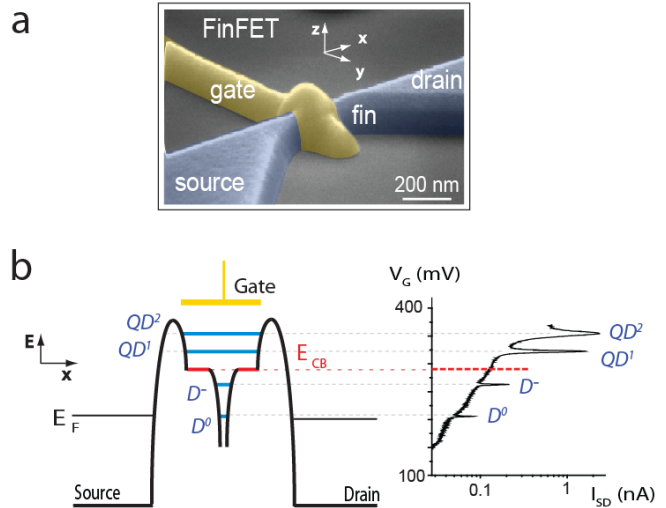
Figure 1. Geometry and electrical characteristics of a single donor located in the channel of a FinFET device. (a) Colored Scanning Electron Micrograph of a typical FinFET device. (b) Band diagram along the x-direction with the D^0-state in resonance combined with the measured source/drain current versus gate voltage for a typical sample. QD^1 and QD^2 indicate resonances of a quantum dot, formed by the confinement provided by the corner effect and residual barriers in the access regions between source/drain and channel. The gate voltage where the band edge in the channel is aligned with the Fermi energy E$_F$ in source/drain, indicated by E$_{CB}$, is estimated by subtracting one unit of addition energy from QD^1. Below the band edge, there are resonances ascribed to the D^0 and D$^-$ charge states of a single donor.

Devices

The FinFET devices used in this study consist of crystalline silicon wires (fins) with large contacts patterned by 193 nm optical-lithography and dry etching from Silicon-On-Insulator, see Fig. 1a After a boron channel implantation, a 100 nm polycrystalline silicon layer was deposited on top of a nitrided oxide (1.4 nm equivalent SiO$_2$ oxide thickness). A phosphorus (P) implant was used for predoping and the structure was subsequently patterned using an oxide hard mask to form a narrow gate. Next,

we used high-angle arsenic (As) implantations as source or drain extensions, while the channel was protected by the gate and 50 nm wide nitride spacers and remains p type. Finally, As and P implants and a NiSi metallic silicide are used to complete the source or drain electrodes. The samples in this research all have a gate length of 60 nm.

Approach

We perform transport measurements on an ensemble of devices at a temperature of 4 K and search for the fingerprints of isolated donors. These single donors are located in or near the active cross-section of the channel, i.e. the cross-section of the FET body where the potential is lowest and the electrical transport thus takes place. Large electric fields induced by the gate or even corners effects can reduce the active cross-section to dimensions much smaller than the FETs body. In our case corner effects play a mayor role indicated by an active cross-section, as determined by thermionic transport measurements, of around 4 nm^2 (5).

A single donors fingerprint is characterized by a pair of resonances in the I_{SD} versus V_G characteristics at low V_{SD} (Fig 1b). The positions of a pair of resonances in V_G are an indication of the energy of the one-electron (D^0) and two electron charge states (D^-). There is a large quantum dot present in the channel (with charge states indicated by QD^1 and QD^2), which allows us to roughly determine the position of the band edge in the active area. While we almost always find a quantum dot in the channel, only about one out of seven devices has an isolated donors fingerprint. The positive identification of the resonances as a donor is based in the determined binding energy, charging energy and the odd-even spin filling (4).

Next we determine the excited energy levels of the one-electron (D^0)-state by sweeping both the V_G and V_{SD} biases and measuring the conductance in the appropriate bias space, see Fig 2. In this so-called stability diagram we observe the typical diamond-shaped region associated with Coulomb-blocked transport between the D^0 and D^- states. The total electric transport in the conducting regions increases as an excited level of the D^0-state enters the bias window defined by source/drain, giving the stability diagram its characteristic pattern (6) indicated by the dashed black lines. The red dots indicate the combinations of V_B and V_G where the ground state is at the Fermi energy of the drain and an excited state is at the Fermi energy of the source. It is the bias voltage V_B in this combination that is a direct measure for the energy of the excited state (e $V_{B,N}$ = E_N), where E_N is the energy relative to the ground state and N is the level index). The excited states as

determined in this fashion are depicted in Table I. These levels are not bulk-like but heavily influenced by the local electric field and the nearby interface (7,8).
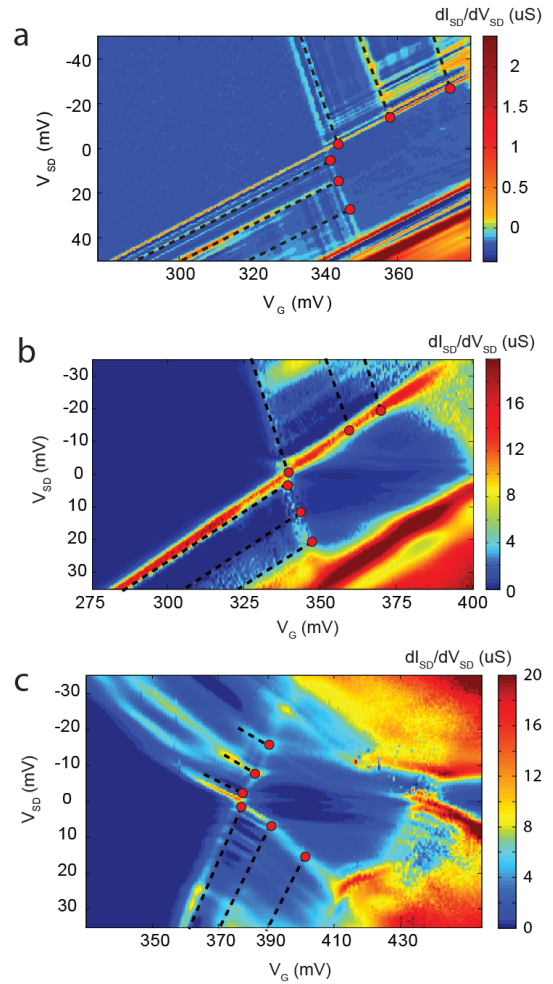
Figure 2. Source/drain differential conductance of the D^0 charge state as a function of bias voltage and gate voltage of a typical single donor FinFET devices. The excited states, indicated by the black dashed lines, form the fingerprint by which we can identify the donor properties. The red dots are a direct indication for the energy of these states ($E_i = eV_{SD}$, with E_i the i-th excited state and e the unit charge.) a) Sample 13G14. Excited states are observed at 3.5, 15.5 and 26.4 meV b) Sample 10G16. Excited states are observed at 2, 15 an 23 meV. c) Sample GLJ17. Excited states are observed at 2, 7.7 and 15.5 meV.

Finally, we compare the measured level spectrum to a multimillion atom tight-binding NEMO 3-D calculation (9) of the system taking two possible chemical species, As and P, into account. NEMO 3-D solves for the eigenvalues of the single electron Schrödinger equation in a tight-binding approach (9). The NEMO simulation package is based on about 14 years of development at Texas Instruments, NASA Jet Propulsion Laboratory, and Purdue University (10). Each atom is explicitly

represented and the electronic structure of the valence electrons is represented by ten sp3d5s* orbitals. Spin can be included explicitly into the basis by doubling the number of orbitals. Spins are coupled through spin-orbit coupling resulting in accurate valence band states. The five d orbitals help shape the curvature of the conduction bands to achieve appropriate masses and symmetries at X and L. The tight-binding parameters that govern the interaction between the nearest neighbor orbitals are tuned to reproduce the bulk Si properties under various strain conditions faithfully. For systems where the primary interest is in the conduction band properties and if no magnetic fields need to be considered, spin can safely be ignored without any significant loss of accuracy. Effects due to crystal symmetry, strain, local disorder, and interfaces are explicitly included in the model through direct atomic representation.

The single impurity states are modeled with a simple Coulomb potential away from the impurity site and central on-site core correction to match experimentally observed bulk-like impurity energies. The simulation domain for a bulk-like single impurity must be large enough such that the hard wall boundary conditions imposed by the finite simulation domain are not felt by the central impurity. With a simulation domain of $30.4 \times 30.4 \times 30.4 nm^3$ corresponding to about 1.4 million silicon atoms the impurity eigenstates move less than a µeV with further domain size increases. A critical modeling capability here is the need to be able to compute reliably the ground states as well as the excited states of the impurity system, as that is a significant component of the impurity fingerprint. Figure 3a shows typical eigenstate spectra for an As donor (two donor depths) and a P donor as a function of electric field. Three electric field regimes can be distinguished (Fig 3b). At the low field limit (F ~ 0 mV/m) we obtain the spectrum of a bulk As donor. In the high field limit (F~ 40 MV/m) the electron is pulled into a triangular well formed at the interface and the donor is ionized. In the cross-over regime (F ~ 20 MV/m) the electron is delocalized over the donor- and triangular well potential
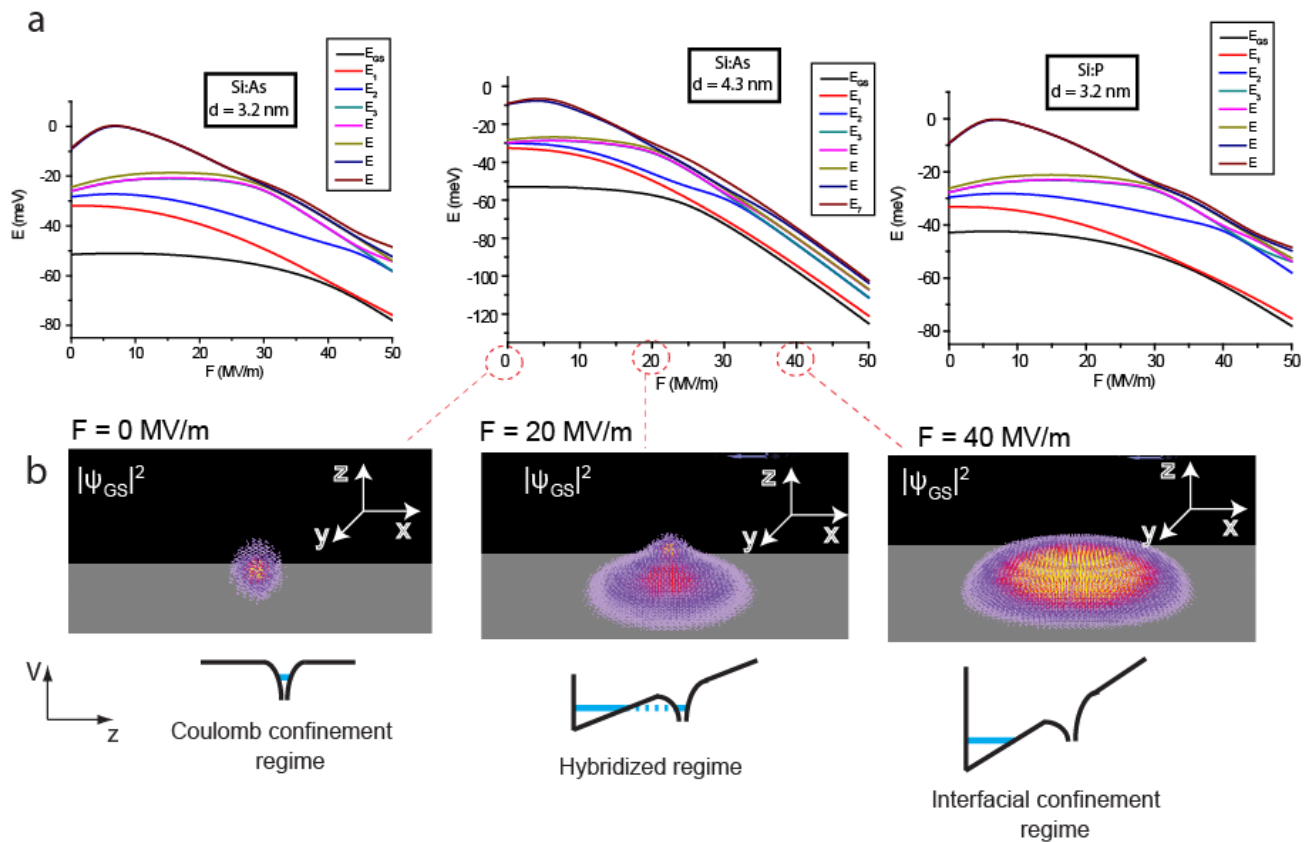
Figure 3. a) First eight eigenlevels of an As donor 3.2 and 4.3 nm below the interface and a P donor 3.2 nm below the SiO₂ interface as a function of electric field (F) calculated in a tight-binding model (NEMO 3-D). Note that we measure excited states relative to ground state (black line in this graph.) b) Calculated wavefunction density of an As donor with d = 4.3 nm for three different fields. The gray plane indicates the SiO₂-interface. From low-fields (where the donor has a bulk-like spectrum) to high fields, the donor electron makes a transition from being localized on the donor to being localized at the Si interface.

and the level spectrum consist of levels associated with the donors, levels associated with the triangular well at the gate interface (formed by the local field) and hybridized combinations of the two (8).

The measured level spectra are least-square fitted to a calculation over a sufficiently sized region of F-d (field and donor depth parameter space. At least three excited levels per donor are taken into account to make the fit over-determined. The fitting procedure is performed for two different species of donor atoms, As and P, which were both used in the fabrication process.

The concentration of donors in or near the active area of the FET channel can be estimated by comparing how many times a single donors is identified with the relevant volume where donors can be found.

Results

We have examined around forty devices and found six where the fingerprint of a single donor showed up in the transport characteristics. These devices were subsequently measured carefully and the D^0 level spectrum was fitted. The quality of the fits, indicated by $\chi2$, across the six samples is 0.92 ($\chi2 < 1$ means a good fit) assuming As donors. For P donors, we find a $\chi2$ of 10.22 (although two of the six are comparable in quality.) Based on the fits, we assume the donors in the active of our devices to be As.

The (over-determined) fit furthermore yields a unique combination of (F, d) for each single donor device, as shown in Table I, together with the measured the level spectra, and their fits.

Finally, we turn our attention to the donor concentration. As mentioned before, the active cross-section of the devices are heavily reduced by a corner effect. The donors we find are in or near these corners, and from the least-square fit we actually know the donor depths range from ~ 3 to 6 nm below the Si/SiO$_2$ interface, see Table I. The part of the FinFET channel where donors are found, a volume spanned by the donor depths and the gate length, combined with a 1:7 success ratio yields a local As concentration of about 10^{18} cm^{-3}

Impact

The excellent quantitative agreement between the measured and modeled level spectra give us good confidence that we can determine the chemical species and local field of single impurities in Si FinFET transistors. Furthermore, the local concentration of donors near the active cross-section of the FinFET can be estimated. The presented method offers opportunities for non-invasive

characterization down to the level of a single donor and could be a future tool in the guidance of device processing.

Table I. First three measured excited states of each sample (see for example fig 2.) versus the best fit to the NEMO 3-D model (as depicted in Figure 3). The fit yields a unique combination of (F, d) for each single donor device. The measurement error for each level is estimated to be around 0.5 meV.

Device		E1 meV	E2 meV	E3 meV	d nm	F MV/m	s meV
10G16	Exp	2	15	23			
	TB	2.2	15.6	23.0	3.3	37.3	0.59
11G14	Exp	4.5	13.5	25			
	TB	4.5	13.5	25.0	3.5	31.6	0.04
13G14	Exp	3.5	15.5	26.4			
	TB	3.6	15.7	26.3	3.2	35.4	0.17
HSJ18	Exp	5	10	21.5			
	TB	4.5	9.9	21.8	4.1	26.1	0.63
GLG14	Exp	1.3	10	13.2			
	TB	1.3	10	12.4	5.2	23.1	0.28
GLJ17	Exp	2	7.7	15.5			
	TB	1.3	7.7	15.8	4.9	21.9	0.77

References

(1) A. Asenov, "Random dopant induced threshold voltage lowering and fluctuations in sub 50 nm MOSFETs: a statistical 3D `atomistic' simulation study" , Nanotechnology **10**, 153-158 (1999).

(2) L.E. Calvet, R.G. Wheeler and M.A. Reed, "Observation of the Linear Stark Effect in a Single Acceptor in Si", Phys. Rev. Lett. **98**, 096805 (2007)

(3) M. Hofheinz, *et al.*, "Individual charge traps in silicon nanowires", Eur. Phys. J. **B 54**, 299 (2006)

(4) H. Sellier *et al.*, "Transport Spectroscopy of a Single Dopant in a Gated Silicon Nanowire", Phys. Rev. Lett. **97**, 206805 (2006)

(5) H. Sellier *et al*, "Subthreshold channels at the edges of nanoscale triple-gate silicon transistors", Appl. Phys. Lett. **90**, 073502 (2007)

(6) L.P. Kouwenhoven *et. al.*, "Mesoscopic Electron Transport", edited by L. L. Sohn, L. P. Kouwenhoven, and G. Schön (Kluwer, Dordrecht, 1997)

(7) M.J. Calderòn, B. Koiler, X. Hu., S. Das Sarma, "Quantum Control of Donor Electrons at the Si/SiO$_2$ interface", Phys. Rev. Lett. **96**, 096802 (2006)

(8) G.P. Lansbergen *et al.*, "Gate-induced quantum-confinement transition of a single dopant atom in a silicon FinFET", Nature Physics **4**, 656 (2008)

(9) G. Klimeck *et al.*, "Atomistic Simulation of Realistically Sized Nanodevices Using NEMO 3-D—Part I: Models and Benchmarks", IEEE TED, **54**, 2079 - 2089 (2007)

(10) G. Klimeck and M. Luisier, "From NEMO1D and NEMO3D to OMEN: moving towards atomistic 3-D quantum transport in nano-scale semiconductors", IEEE IEDM 2008